An Accurate Detection for Dynamic Liquid Level Based on MIMO Ultrasonic Transducer Array

Peng Li, Yulei Cai, Xiaolong Shen, Sharon Nabuzaale, Jie Yin, and Jiaqiang Li

***Abstract*— In many circumstances, the conventional ultrasonic liquid-level detection presents the unreliable estimations due to the dynamically changed liquid level. In addition, there are circumstances where the level change involves not only the fluctuation but also the rise or fall of liquid level. To improve the measuring accuracy of liquid level using the ultrasonic method in dynamically changed level case, an attractive ultrasonic method, named the liquid-level detection based on the multiple-input multiple-output ultrasonic transducer array, is proposed in this paper. This method is different from the early ultrasonic liquid-level detections, including those that utilize transducer array. Based on the virtual element technology, the method employs the multitransducer array to achieve the reduction of system complexity and cost, and then applies the synthetic aperture technology to realize rapid samples of liquid level. Besides, one adaptive searching scheme of focused position in beamforming of synthetic aperture in each scanning direction is optimized to get the high precise samples of liquid level. The proposed method is verified by simulation and a real system, and compared with the conventional single-channel approach. We still proposed a simulation method of ultrasonic echo signal from liquid level based on the boundary-layer theory and the ultrasonic scattering theory. The simulated and actual measurement results demonstrate that the proposed method is obviously superior to the conventional approach. Meanwhile, the factors influencing on the proposed method are investigated by simulation also. The investigations reveal that the focus position in beamforming, the SNR of echo signal, and the wave size of liquid level have impact on the suggested method. However, it is indicated that the good performance of the proposed method remains, provided that the focus in beamforming is properly set in every scanning direction and the noise of echo signal is effectively controlled.**

***Index Terms*— Acoustics, arrays, level measurement, measurement errors, multiple-input multiple-output (MIMO) systems, transducers.**

I. Introduction

THE accuracy of liquid-level detection is a key aspect for many applications, such as oil, chemical, meteorological industry, and so on. A variety of principles have been existed, including mechanical, optical, electrical, electromagnetic, and ultrasonic methods. These methods have achieved certain progress on the liquid-level measurement. The mechanical method mainly uses a buoy floating on the liquid to measure the liquid level. The buoys position can be measured by sliding resistance, radar, or a single digital camera [1], [2]. The mechanical method can be easy to implement, but there is a limit about the kind of liquid and a larger error because of posture of the buoy. The optical fiber liquid-level measurement is realized by monitoring the valley wavelength shift or the intensity of optical fiber [3], [4]. Compared with the other traditional method, the fiber optic has the advantage of high sensitivity, strong antielectromagnetic interference capability, corrosion resistance, and compact size [5]. However, current fiber optic level sensors share common disadvantages, including small measurement range and complex mechanical structure. Electromagnetic liquid-level measurement is mainly based on the absorption or reflection of measured liquid to determine the height of liquid level [6]–[8]. Different media have different degree of absorption for electromagnetic wave. When using this feature, the liquid level can be measured from different media. Besides, the reflection characteristics of electromagnetic wave can be used to measure the time-of-flight, and then calculate the liquid level. However, electromagnetic wave has a larger attenuation, the measuring distance is shorter, and the cost is higher. Electrical methods are mainly composed of capacitor methods. The conventional capacitance-type level sensor is based on the linear relationship between the capacitance and the liquid level to measure the liquid level [9], [10]. The presented sensor has the advantages of low cost, low energy, good repeatability, and high linearity. In addition, this sensor can be used to detect the water level regardless of water type with adding the reference electrode plate, hence it could trace the rising tide of the water level instantly [11], [12]. However, the hysteretic problem in dynamic response still be exist. In addition to that, further studies on robustness, lifetime, and the environmental condition are needed to achieve better processing time of measuring liquid level in the case of turbulent flow [11]. In addition, assisted with a high-resolution 3-Mpixel CMOS camera and a hardware digital image processor implemented in a field-programmable gate array (FPGA), a new high-precision automatic measurement system for liquid-level measurement has been presented in membrane distillation application [13]. The system is simple and low coat compared with a common measurement system.

The ultrasonic method is widely applied to liquid-level detection because of its higher cost performance. Evolved over

Manuscript received February 21, 2014; revised July 26, 2014; accepted July 26, 2014. Date of publication September 26, 2014; date of current version February 5, 2015. This work was supported in part by the National Natural Science Foundation of China under Grant 41075115, in part by the Natural Science Foundation, Jiangsu Higher Education Institutions of China, under Grant 10KJB510012, in part by the Jiangsu Overseas Research and Training Program for University Prominent Young and Middle-aged Teachers and Presidents, and in part by the Priority Academic Program Development, Jiangsu Higher Education Institutions. The Associate Editor coordinating the review process was Dr. Subhas Mukhopadhyay.

The authors are with the Jiangsu Key Laboratory of Meteorological Observation and Information Processing, Jiangsu Technology and Engineering Center of Meteorological Sensor Network, Nanjing University of Information Science and Technology, Nanjing 210044, China (e-mail: lipengdcy@nuist.edu.cn).

Color versions of one or more of the figures in this paper are available online at http://ieeexplore.ieee.org.

Digital Object Identifier 10.1109/TIM.2014.2357586

the years, we can see these significant improvements mainly in some areas, such as transmitted signal optimization, echo characteristic utilization, time-of-flight estimation, and received signal processing. Here, the several corresponding examples are provided for these aspects of improvement. The propagation attenuation and reflectance rate of ultrasonic wave can be analyzed and utilized to accurately estimate the liquid level [14], [15]. The ultrasonic lamb wave is transmitted along the tank wall to effectively detect the liquid level [16]. In time-of-flight estimation, the unscented Kalman filter is applied to the received signal to estimate the echo envelops as well as accurately locate its onset [17], [18]. In addition, other strategies estimating the time-of-flight in ultrasonic range detection can be absolutely applied to the level detection and completely obtain a higher estimation accuracy because the ultrasonic level detection is essentially a kind of range sensing [19]–[22]. In signal processing, first, an adaptive filter is used to remove the noise and interference in echo signal, and then the cross-correlation method is applied to identify the time-of-flight to obtain precise level estimation [23].

However, in practical application, the irregular change of liquid level may result in a poor performance for the liquid-level detection methods above, because sometimes the liquid level is dynamically changed, especially those level change involves not only fluctuation of liquid surface but also rise or fall of liquid level. Therefore, many methods have been developed for the dynamically changed level detection. For example, the online support vector regression algorithm is presented to be a solution to measure the dynamic liquid level. This method not only has good performance, but also can update the forecast model by online [24]. The optical method, through the analytical expressions that include the relationship between optical intensity and liquid surface sloshing wave and the expressions of the wavelength as well as amplitude, can obtain the optical patterns corresponding to static and sloshing liquid surface. Then, the sloshing variation process, including rising and damping, can be achieved. The detection is nondestructive and real time [25].

The conventional single-channel ultrasonic method is also used to the changed liquid level by repeating level measurement many times and averaging the measured values. Nevertheless, this simple way is only restricted to the case that the liquid level is fluctuated but not involve the rise or fall of liquid level. In addition, one approach is based on a plurality of transducers. In this scheme, the ultrasonic waves with different carry frequency are emitted in some predetermined directions from some positions below the liquid surface, and echoes are received by corresponding transducers to determine the level values at different positions on the whole liquid level, and then the final level estimation can be obtained by averaging these level values [26]. However, the complexity and cost of this method will go up following the sampling number of liquid-level increase. The other method employs the support vector machine signal processing and the classification scheme to realize the accurate level determination [27]. This method also has difficulty to adapt the rapid changed liquid level due to its complicated calculation.

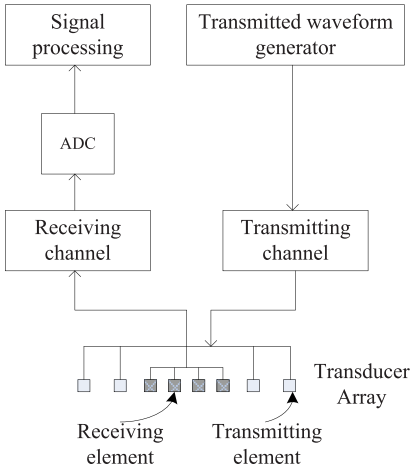

Fig. 1. Architecture of ultrasonic measurement for dynamic liquid level based on MIMO transducer array.

The reason that we are interested in the accurate measurement of changed liquid level is to achieve the accurate rainfall gauging by ultrasound in the case of heavy rain. When implementing rainfall gauging in meteorological observation, the dynamically changed liquid level will appear due to the collected rain pouring into the measuring container. It is a challenging work to reach an expected level detection by ultrasound under the circumstances. Therefore, we proposed an ultrasonic approach to achieve this goal. In this paper, the linear ultrasonic transducer array is designed and the scanning of liquid level is implemented in our approach. This way, the spatial sample of liquid level can be realized and the accurate estimation of level can be reached by averaging the level samples. To accurately sample liquid level with a simple and low-cost ultrasonic approach, we refer to the new relevant findings in radar research, and propose a distinctive liquid-level measurement approach that is based on the multiple-input multiple-output (MIMO) ultrasonic transducer array. The proposed approach is still composed of several relevant parts: transducer array, signal transmitting and receiving channels, and signal processing unit. The architecture of ultrasonic measurement for dynamic liquid level based on MIMO transducer array is shown in Fig. 1. However, it is essentially different from conventional phased array approach. The transducer array is designed to form the virtual phase array structure, thus the complexity and cost of system can be considerably reduced by the virtual element technology. In signal processing, the synthetic aperture technology can be used to realize rapid sample of any position on the liquid level. Besides, the adaptive searching of focal position in every sampling direction is optimized to get the high-precise samples of liquid level. Furthermore, the linear Frequency Modulated Continuous Wave (FMCW) pulse is optimized to serve as transmitted signal.

II. Proposed Method and Its Key Aspects

A. Transducer Array Architecture

According to the MIMO phased array radar scheme [28], the M transmitting transducers and N receiving transducers

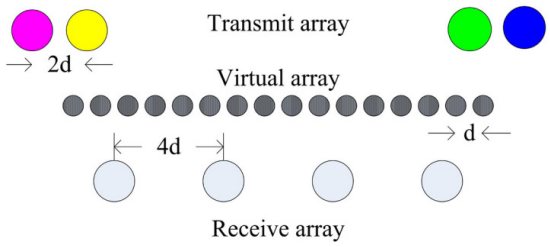

Fig. 2. Illustration of linear MIMO array design with four transmit elements and four receive elements.

of the proposed approach are arranged as a linear array. This arrangement is concretely that the receiving transducers are in the middle of array and the transmitting transducers divided into two groups surrounding the receiving transducers. Assuming that $M = 4$ and $N = 4$, the transducers are arranged into a linear array in terms of certain rules, and a uniform linear array of 16 virtual transducers will be synthesized. It means that a desired pattern of virtual phased array can be generated by properly arranging the placements of transmitting and receiving transducers [29]. Fig. 2 shows an illustration of the arrangement of ultrasonic transducers forming a linear MIMO array. As observed from Fig. 2, this is a symmetrical array architecture. To determine the placements of all actual transducers and virtual transducers, it is necessary to set a coordinate system, in which the array center is the origin of coordinates and the center line of transducers overlaps with the x-axis of coordinate. If a uniform linear virtual array with nonoverlapping equal spacing d is demanded, the actual transducers of the coherent MIMO transducer array are placed as the following designing rules: the spacing between the transmitting transducers is $d_t = 2d$, the spacing between the receiving transducers is $d_r = Md$, and the gap between each $M/2$-transducer transmitted group and the edge transducer of the receive array is $d_{\text{tr}} = d$. The physical length of the designed MIMO transducer array is $(MN + M - 2)d$, and the length of the virtual array is $(MN-1)d$. It is notable that the coupling effect of transducers is not to be considered here.

Considering that the diameter of round transducers employed in actual system is 12 mm, we set d equaling to 15 mm. Therefore, the physical length of linear transducer array is about 282 mm, and the length of the virtual array is about 225 mm. If the beam angle of the transmitting transducer is 20°, the ultrasonic irradiation range is about 868 mm along the x-axis of coordinate when the distance between array and liquid level is 1000 mm. In addition, it is not necessary to consider the appearance of grating lobe because the spacing of formed virtual array is more than the required distance of 0.5 λ in the conventional phased array. According to the scheme above, there are $M \times N$ different propagation channels from the transmit array to the receive array. If the receive array can identify the transmit source of received signal, we can obtain a virtual phased array of $M \times N$ elements only using $M + N$ actual elements [30]. Comparing with the conventional phased array, $(M \times N) - (M + N)$ elements or propagation channels can be saved. This virtual array element technology is actually beneficial to achieve our purpose of reducing the system complexity and cost.

B. FMCW Signal Model

The diversity of the coherent MIMO detection system can be achieved by employing time-division multiplexing, frequency-division multiplexing, spatial coding, and orthogonal signal [31]. In this paper, we choose the FMCW pulse as the transmitted signal, because the FMCW technology allows a low-cost and compact system design and also enables relatively low sampling rates. Besides, the FMCW pulse signal has a large-time bandwidth product and can improve the range resolution. These advantages of FMCW technology can achieve our aim to lower the complexity and cost of system. In addition, the FMCW technology has been successfully applied in the sparse coherent MIMO radar [28], [29], [31]–[34], and the relevant technologies can be referenced to the proposed approach.

The FMCW pulse signal of transmitting transducer is given by the following form:

$$s_t = \exp\{j(2\pi f_c t + \pi K t^2)\}, \quad |t| \le T_c/2 \tag{1}$$

where T_c is the duration of pulse, f_c is the carrier frequency, K is the chirp rate defined by the bandwidth B and the pulse duration T_c of the transmitted signal, i.e., $K = \pm B/T_c$. Positive K represents up-chirp, and negative K stands for down-chirp. Usually, the duration of transmitted FMCW pulses is not overlapped, that is, the pulse repetition frequency (PRF) $\le 1/T_c$. However, we determine the PRF in terms of the specified maximum range $R_{\max}$ or the maximum time $T_{\max}$ that the ultrasonic wave reaching the maximum detected range and returning the receiving transducers, namely PRF $\le 1/T_{\max} = c/2R_{\max}$. Here, c stands for the speed of sound.

The received signal can be modeled by

$$s_r(m, n, t) = \int_{R_{\max}} \alpha(p) A_r(p; m, n, t) s_t\left(t - \Delta t_{m,n}\right) dp \tag{2}$$

where $m, n \in N$ is the transducer index of transmitting and receiving array, respectively, α is the reflectivity function, $p \in R_{\max}$ is the point target in the illuminated region, A_r is the amplitude function of sound wave, and $\Delta t_{m,n}$ is the time delay of FMCW pulse signal from the mth transmitting transducer x_m to the point target p and back to the nth receiving transducer x_n

$$\Delta t_{m,n} = d_{p;m,n}/c = (|p - x_m| + |p - x_n|)/c \tag{3}$$

where it is emphasized that the proposed method is limited to the near-field condition instead of the far-field condition [29], [35]. Because there is no constant approximate angle θ with respect to the boresight, the range of sound wave propagating from each virtual element $x_{m,n}$ to the point target p can be not expressed simply as $d_{p;m,n} = 2R_p + 2x_{m,n}\sin\theta$ [28], especially when the point target p locates very close to transducer array, where R_p is the range of point target from the transducer array.

After applying the deramp technique and a low-pass filtering to the received signal, the resulting signal is modeled by

$$s(m,n,t)=\int_{R_{\max}}\alpha(p)A_r(p;m,n,t)\exp\{j2\pi\phi(p;m,n,t)\}dp. \tag{4}$$

Then, the partial derivative of phase function can be provided as follows:

$$\frac{\partial\phi}{\partial t}=K\Delta t_{m,n}. \tag{5}$$

Because the partial derivative of the phase function of a certain signal corresponds to its frequency composition, we can get the frequency expression of the signal received by virtual transducer $x_{m,n}$, that is, $f_{m,n}=K\Delta t_{m,n}$, which includes the range information of the target. Therefore, the range of sound wave propagates from the transmitting transducer x_m to the target and then back to the receiving transducer x_n, or the range between the virtual element $x_{m,n}$ and the target can be calculated by

$$d_{p;m,n}=cf_{m,n}/K=c\Delta t_{m,n}. \tag{6}$$

As can be seen from (5) and (6), both range and bearing information are included in the phase function after the deramp processing. This also implies that we can effectively determine the range of target after deramping the received signals and converting the time delay into the frequency domain. In addition, we still observe from (7) that $f_{m,n}$ and $d_{p;m,n}$ are different along with the variation of the time delay $\Delta t_{m,n}$. Therefore, the phase of received signal can be changed by adjusting the time delay. This is the basis of time-domain beamforming in MIMO-based FMCW imaging technology.

To differentiate the transmit channels in the synthesization of $M\times N$ MIMO channels, the time division scheme is frequently used to switch the transmitting channels ON or OFF for radiation at different time slots. With the time-division transmission, the transmitting transducers are activated in turn while all receiving transducers receive echo signals synchronously. The reception of transmitted signals for all slots makes a round of scan, and a total of $M\times N$ channels of signals are obtained. In this paper, we still employ this simple but reliable signal transmission scheme. Considering the four transmitting and four receiving transducers in Section II-A, the signal transmission scheme is described by a time–frequency diagram in Fig. 3. When implementing this scheme, the time slot is determined according to the maximum detection range, and the boundary of chirp duration is ensured in terms of the condition $T_M<\lambda/(4(M-1)v)$ and less than the time slot, where T_M is the maximum duration and v is the velocity of the target. Meanwhile, it is necessary to comprehensively consider resolution, echo power, acceleration and velocity of the target, and so forth.

C. Digital Beamforming Algorithm

Many methods of digital beamforming (DBF) have exited [28], [29], [36]–[40]. In this paper, we still consider the conventional time-domain DBF algorithm. Based on the symmetrical array architecture described above, we first set a coordinate to be beneficial to calculate the time delay of every virtual transducer before implementing the DBF. Because we mainly consider the cross section scan in 2-D, a 2-D coordinate system is set to determine the corresponding locations of all array transducers, as shown by Fig. 4. In the coordinate system, x-axis overlaps with the center line of transducer array and the transducers are symmetrical to the z-axis, and z-axis is the propagate direction of ultrasound wave. In Fig. 4, supposing that the point P is a desired spatial sample on the liquid level, it is regarded as the point target. Thus, it is also the focus position in beamforming. Assuming that the coordinate of point P is known, the orientation from the origin of coordinate system to the point P is considered as the direction of synthetic ultrasonic beam or the scanning direction. In addition, the angle θ between the axial direction of synthetic beam and z-axis is regarded as the azimuth angle.

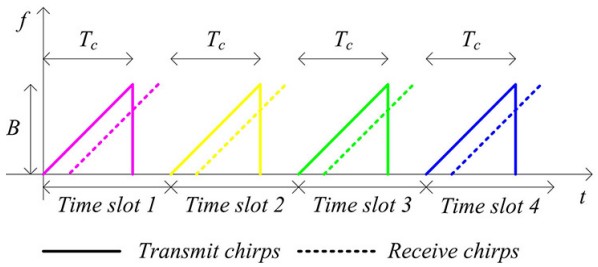

Fig. 3. Transmission scheme for an array of four transmit elements.

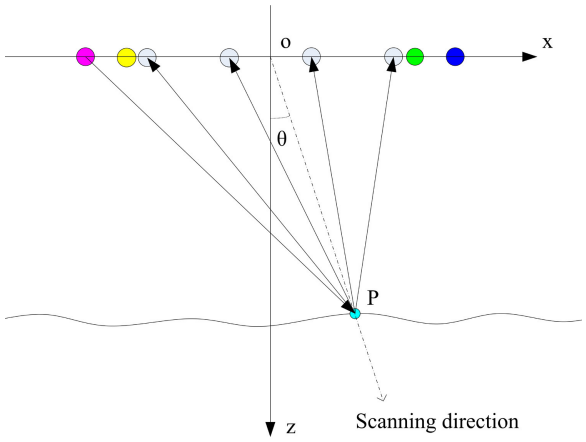

Fig. 4. Illustration of arranged array with four transmit elements and four receive elements.

According to the coordinates of all transducers in array and the point target, the time delay of each virtual transducer can be achieved in terms of (3). However, these time delays are compensated with different relative time delays $\tau_{m,n}$, that is, $\Delta t_c=\Delta t_{m,n}+\tau_{m,n}$, in where $\tau_{m,n}$ stands for the time difference of wave propagation from the reference point to every transducer in virtual array. Δt_c is the time from the transducer array center to the target P and back to the array center. Δt_c is a constant because of the compensation of $\tau_{m,n}$. Thus, the signal after beamforming can be written as follows:

$$s_r(t)=\sum_{m,n}\int_{R_{\max}}\alpha(p)A_r(p;m,n,t)s_t\left(t-\Delta t_c\right)dp. \tag{7}$$

Because the echo signals are sampled in the receiving process, we can numerically implement the time-delay sum and deramp. Following the low-pass filtering, a frequency down-converted signal can be obtained to estimate the target range. Thus, the distance between the center of transducer array and the point P can be calculated by

$$d_{o,p} = c\Delta t_c/2. \tag{8}$$

D. Dynamic Liquid-Level Detection

After receiving all echo signals, the total four receiving channels of data are reorganized into 16 channels of echo signals, each of which corresponds to a virtual phase array transducer. On this basis, we implement the related signal processing and estimate the liquid level. In summary, the implementing of dynamic level detection mainly includes several steps. In the first place, determine the focal position of DBF or synthetic wave beam in a certain scanning direction. From Fig. 4, we can see for a fact that the location of spatial sample P on liquid level changes randomly and the focal position of DBF has a small probability to overlap with the sample P. Therefore, the focal position deviation from the sample P is one of the main reasons giving rise to the sampling error, and this will be proved in the simulation section below. For this reason, it is necessary to correctly determine the focus position. Our consideration is first to obtain a rough level value utilizing the received signals $s_r(2, 1, t)$ or $s_r(3, 4, t)$ corresponding to the virtual transducer $x_{2,1}$ or $x_{3,4}$ before performing the DBF, and then a range of focal position will be determined according to this rough level estimation. For another, determining focal position and sample value of liquid level in predetermined scanning direction. Some points along the predetermined direction in the focus range are supposed as the potential focal points. We implement the DBF and the pulse compression processing for each potential focal point. When the amplitude of the main lobe of the compressed signal reaches the maximum value, the corresponding position of the potential focal point is the expected focal position, and the sample value in this direction can be obtained by the range from focal position to array center and the azimuth angle θ. One needs to alter the scanning direction and repeat the process until the focal position and sample in each predetermined direction are attained. Finally, the accuracy measurement of liquid level can be achieved by averaging the samples in all directions. The total implementing process of proposed approach for the estimation of changed liquid level can be explicitly described by the block diagram shown in Fig. 5.

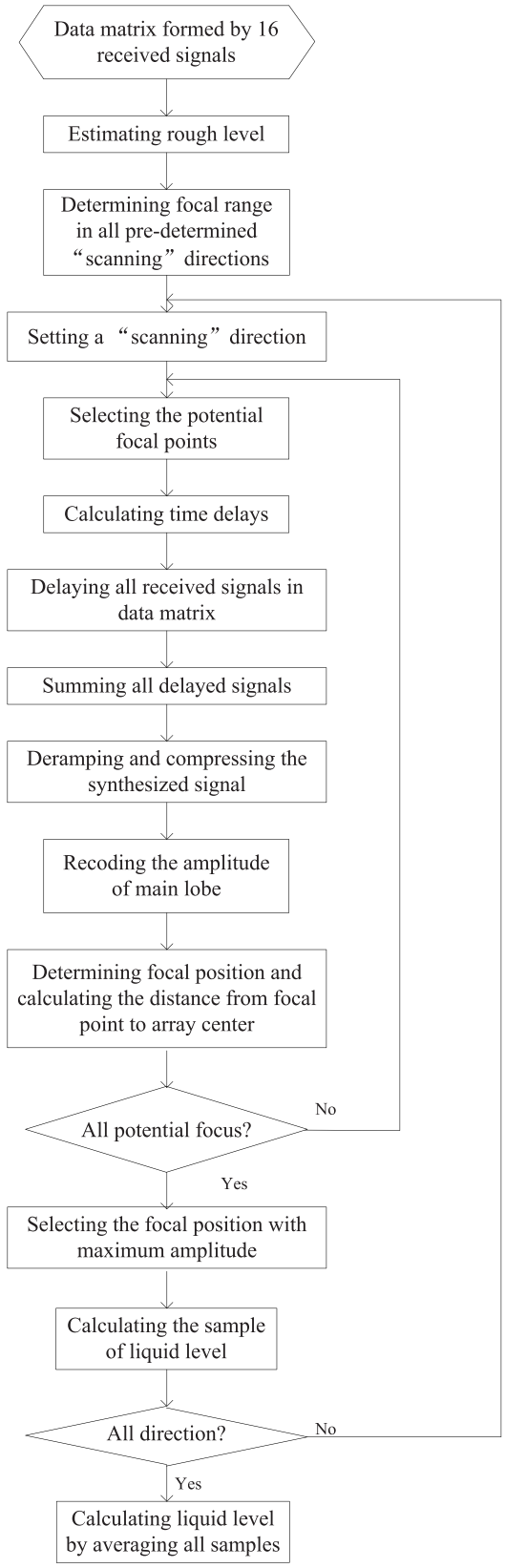

Fig. 5. Illustration of total implementing process of the ultrasonic level detection with MIMO-based array.

III. Verifications Using Simulated Signals

We will verify the feasibility of our approach by simulation in this section. Simultaneously, the proposed approach is compared with the conventional signal channel detection. In addition, we still examine the influence of some relevant factors on the method, such as the focal position in beamforming, the SNR of echo signal, and the wave size of fluctuated liquid level. The relevant simulation results are analyzed with the aim of further improving the proposed method.

A. Simulation of Echo Signal

The simulation of echo signal from a liquid level is a very hard work, because the air–water interface of liquid level is

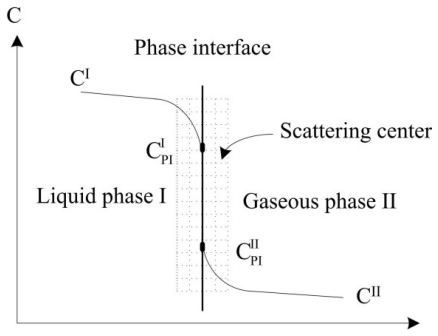

Fig. 6. Description of concentration difference of water molecules in phase interface.

very complex. Based on the boundary-layer theory [41], the water and air molecules will certainly encounter resistance when diffusing toward the phase boundary. Therefore, the concentration difference of water molecules will be formed near the air–water interfaces. The change of interface concentration is shown in Fig. 6. In simulating the echo signal from liquid level, for simplicity, we make some small grids on both sides of the phase interfaces, every grid is considered as an independent scatter center of point target, and the scattering intensity of every scatter center is set by the concentration of water molecules, as shown in Fig. 6. When ultrasound irradiates the liquid level, the echo signal is the summation of returned signals from every scatter center in the radiation zone. According to the ultrasonic scattering theory [42], this way is feasible for large detection target. Then, the main work is to build the signal model returned from single point target.

There exists several simulation methods of ultrasonic echo signal [19], [27], [43]. One of these models only involves several fundamental factors, and is widely employed in ultrasonic imaging and detection researches [27], [43]. Because this model is capable of representing the observed signals for a wide variety of target types and locations, we refer to this model and modify it by replacing the monosinusoidal signal with the FMCW pulse signal. Thus, the echo signal of transmitted FMCW pulse from a point target can be approximated by

$$s_r = a_0(t-\Delta t)^2 \exp[-a_1(t-\Delta t)]u(t-\Delta t) \times \exp\{j(2\pi f_c + \pi K(t-\Delta t)^2)\} + w(t). \quad (9)$$

This model is simply an FMCW pulse, and it is enveloped by a function that is the product of a parabola and exponentially decaying function. Here, a_0 and a_1 are the shape and amplitude parameters of the signal, $u(t-\Delta t)$ is the unit step function delayed by Δt, the time delay Δt corresponds to the time that ultrasonic wave from transmitting transducer to target and return back to receiving transducer, $w(t)$ is white Gaussian noise having zero mean and variance σ_μ^2, and the noise may include thermal noise, acoustic noise, amplitude quantization error, and so on.

Considering that the ultrasonic beam is similar to a flashlight beam, its cross section is a circular pattern in which the wave intensity is strongest in the center. Therefore, the sound pressure has to reduce along with the radius increase in wave beam cross section on the basis of energy conservation. Moreover, we consider the configuration with a pair of identical transducers, in which one transducer acts as the transmitter and the other as the receiver. By the reciprocity principle, the amplitude of echo signal from a point target within the radiation zone of ultrasound is weighted by the following [43], [44]:

$$W(r_1, r_2, \theta_1, \theta_2) \cong \epsilon \frac{A_0 r_0^{3/2}}{r_1 r_2^{1/2}} r^{\frac{-(\theta_1^2+\theta_2^2)}{2\sigma_T^2}} \quad (10)$$

where $r_1, r_2 > r_0$, r_1 and r_2 are the distance between the target and transmitting and receiving transducer, respectively, θ_1 and θ_2 are the angular deviations from the center of the transmitted wave and the reflected wave from the target, respectively, and σ_T is the beam-width parameter. For simplicity, $r_0 \cong 10$ cm and $A_0 = 1$.

According to the signal model of single target, we simulate the echo signals from the static liquid level in a single-channel detection system, and we set the relevant parameters shown in Table I according to the actual ultrasonic level measurement. Besides, the coordinates of all transducers are set by Table II. The distance from the transducer array to the liquid level is supposed as 600 mm, that is, the distance to the phase interface. The radiation zone is a shape of round pie with a radius of 200 mm, and is made up of two layers of water–air film with different concentration of water molecules and one layer of water. Every layer is divided into some grids, and every grid represents the scattering center of isolated point target. The size of every grid is 2 mm × 2 mm. Besides, we use the variance to describe the small difference of scattering intensity of every scattering center in same layer. The relevant parameters of radiation zone on liquid level are set as follows: the scattering intensity of scattering center in water

TABLE I
SIMULATION PARAMETERS

Parameters	Value	Unit
Carrier frequency	300	KHz
Bandwidth	60	KHz
Pulse width	2	ms
Detection range	2.04	m
Sound speed	340	m/s
Sample frequency	2.5	MHz
Beam angle	$\pi/9$	rad
Shape parameter	10^7	
Amplitude parameter	10^5	

TABLE II
COORDINATES OF ISOLATE POINT TARGET AND ARRAY ELEMENTS

Target or elements	x-axis(mm)	z-axis(mm)
Transmitting element 1	-72	0
Transmitting element 2	-56	0
Transmitting element 3	56	0
Transmitting element 4	72	0
Receiving element 1	-48	0
Receiving element 2	-16	0
Receiving element 3	16	0
Receiving element 4	48	0

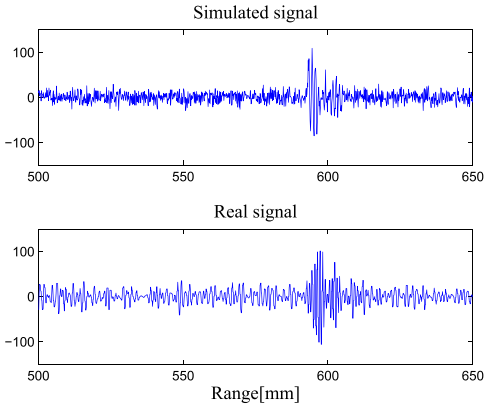

Fig. 7. Wave shape of real and simulated echo signal returned from static liquid level.

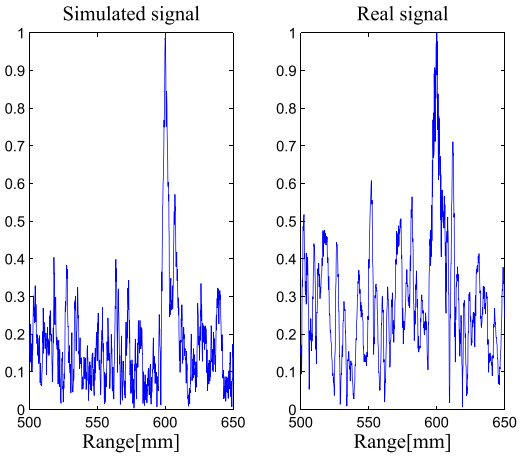

Fig. 8. Compressed signals corresponding to the real and simulated signal.

(liquid phase), water–air film I, water–air film II, and air (gaseous phase) is 0.95, 0.70, 0.35, and 0.05, respectively, and their variance is uniformly as 0.0025. The real and simulated echo signals form liquid level are shown in Fig. 7. After the pulse compression processing with FFT, the compressed signal of two signals are shown in Fig. 8. According to Figs. 7 and 8, it is easy to obverse that the wave shape of two signals are similar, and that the characteristics of main and side lobe of their compressed signals are very similar too. It indicates that our simulating method of echo signal from the liquid level is feasible and the simulated signals can be used to verify the proposed approach.

Besides, we still simulate the 16 channels of echo signal from static liquid level according to the transducer array above; the signals corresponding to the virtual transducer $x_{1,1}$, $x_{1,4}$, $x_{2,3}$, and $x_{3,4}$ shown in Fig. 9 to prove the signal simulation method are also valid for our formed transducer array. From Fig. 9, we can easily see that the FMCW pulse in echo signal is different in amplitude and return time due to the different relative locations between scattering centers and transducers. For the signal amplitude differences, the major reason is that the scatting center locates the different positions on the cross section of the wave beam when the different transmitting transducer illuminates. Then, all 16 channel signals implement the

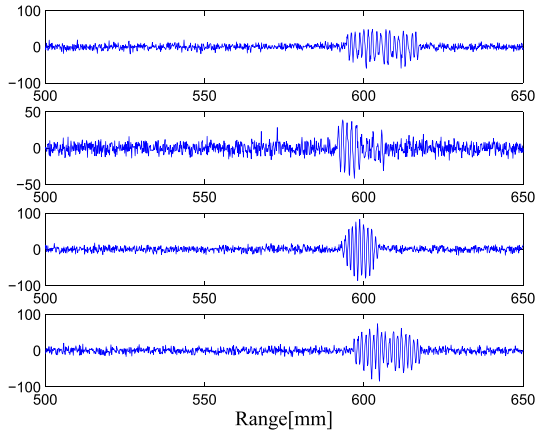

Fig. 9. Simulated echo signal waveforms from the static liquid level corresponding to the virtual element $x_{1,1}$, $x_{1,4}$, $x_{2,3}$, and $x_{3,4}$ separately.

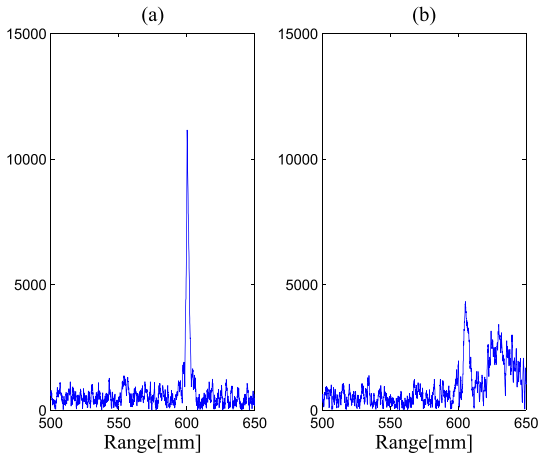

Fig. 10. Compressed signals of synthesized signals. (a) With right time delay. (b) Without time delay.

DBF and the synthesized signal performs pulse compression. When implementing time delay and summation of all signals, the focal position is set at the cross point of phase interface and scanning direction of wave beam. This compressed signal is compared with the compressed signal of directly summation signal without time delay, as shown in Fig. 10. We can see that the compressed signal with time delay has a very high main peak-to-side lobe ratio, and the main lobe has a very narrow width and precisely corresponds to the range to the phase interface of liquid level. The results in Fig. 10 give proof that the conventional time-domain DBF is feasible and can obtain an expected result.

Finally, we perform the simulations of echo signals from the fluctuated liquid level. To get the echo signals reflected from the fluctuated liquid level, a wave curve is generated first to imitate the air–water phase interface of fluctuated liquid level. Both sides of this curve have a water–air film with different scattering intensity, respectively. Using the exact same approach in the previous static liquid level, the echo signals are exactly reflected from scattering centers on the fluctuated liquid level. For the sake of simplicity, we generate an approximate sine-wave curve to represent the phase–air

interface of changed liquid level with the following parameter settings: the period of wave curve is 2, the amplitude of wave curve is 20 mm, the length of ultrasound radiation zone is 800 mm, and the distance of liquid level is 1000 mm when the liquid level is calm. Here, it should be noted that the distance of liquid level is the range between the transducer array and the liquid level. When 16 channels of data are collected, the liquid-level samples can be obtained by implementing the relevant signal processing.

B. Estimation Results

First, we perform the simulation estimation of static liquid level according to the implement process described in Fig. 5. In the simulation, the range from transducer array to liquid level is set as 1000 mm, and the SNR of echo signal is 10. Besides, the estimated result is compared with that of the conventional single-channel detection approach. To keep things simple, the signal corresponding to the virtual transducer $x_{2,1}$ or $x_{3,4}$ is regarded as the received signal of the conventional approach. Furthermore, the placements of transmitting and receiving transducer are considered to reduce the estimate errors when using the conventional approach. According to the implement process, the rough level value is obtained by the signal of $x_{2,1}$ or $x_{3,4}$ and is 1000.31 mm. Therefore, the range of focal position is determined as 1000.31 ± 10 mm due to the static liquid level. The step size of per 2 mm is used to determine the potential focal position along the scanning direction in the range of determined focal position. The estimated results of the proposed and the conventional approach are 999.77 and 1000.31 mm, respectively, and the corresponding absolute errors are only 0.23 and 0.31 mm. This simulation indicates that the two approaches have not the obvious differences in static liquid-level case.

Second, we continue to simulate the fluctuated level estimations. Similarly, the conventional approach is also compared with our approach. The measuring result of the conventional approach is 1005.23 mm, and is also the rough level estimation because they are calculated by the signal of $x_{2,1}$ or $x_{3,4}$. Therefore, the range of focal position is set as 993.61 ± 40 mm, considering the wave amplitude of 20 mm. Besides, the sampling density or the number of sample points per unit length in changed level measurement is considered according to the cross-range resolution and the spatial sampling theory [28], [45]. Here, the sample number per unit length of 100 mm is directly designated as 10 and the whole range of measured liquid level has 80 sample points in total. Using the same solution to find the focal position in every scanning direction, the samples on the liquid level in different directions can be realized. The final level estimation is 999.8 mm, and the maximum error and the variance of level samples are 0.2598 and 0.7477 mm, respectively. The relevant results including the level sample estimations and the corresponding estimating errors are shown in Fig. 11 to further demonstrate the feasibility of proposed method. From Fig. 11, it can be easily observed that the curve shaped by the level sample estimation almost coincides with the water–air interface of the assumed liquid level. In addition,

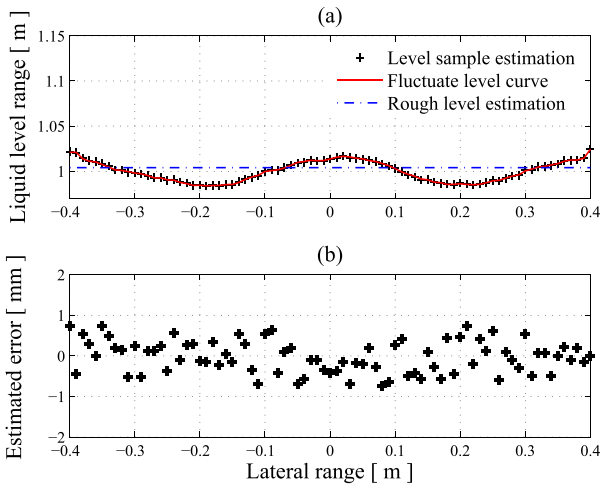

Fig. 11. Simulation results of fluctuated level estimation. (a) Assumed fluctuated liquid level and the level sample estimation. (b) Level sample estimating errors.

the estimation error of level sample is irregularly changed and the errors of sample are very small. This simulation also implies that the searching method of focal position is effective and reduces the influence on the liquid-level sample. Therefore, the simulation results are in agreement with the fact that highly reliable estimation can be achieved by our approach under the changed liquid-level condition.

C. Verification of Influence Factors

In this paper, we still examine several relevant factors influencing on the proposed approach, including noise, focal position, wave size of liquid level, and so on. For the examination of noise effect, we mainly consider the static liquid-level case above. Thus, the SNR of received signal is changed by adjusting the scatting intensity of air in echo signal simulation. Because each transducer is located in the different position, the SNR of signal received by each virtual transducer may not be equal. As before, the simulated signal corresponding to virtual transducer $x_{2,1}$ or $x_{3,4}$ serves as the received signal of the conventional approach. Another advantage to this is that the two methods basically keep an identical noise level. In this verification, the SNR of echo signal is changed from -20 to 25 dB.

The examination results related to the noise effect are shown in Fig. 12. We can observe from Fig. 12 that the two methods do not have obvious differences at high SNR from 16 to 25 dB, and the maximum errors of two approaches are not more than 0.65 mm. However, the proposed method significantly prevails over the conventional approach at medium SNR from 0 to 16 dB. As the SNR of echo signal further reduces, the conventional method becomes completely invalid. However, our method still keeps the smaller measuring error below 1.85 mm even if the SNR of echo signal is from -10 to 0 dB. The experimental results demonstrate that our method is superior to the conventional method in the antinoise performance. The examination is very important to us, because the application of the proposed method in rainfall gauging is

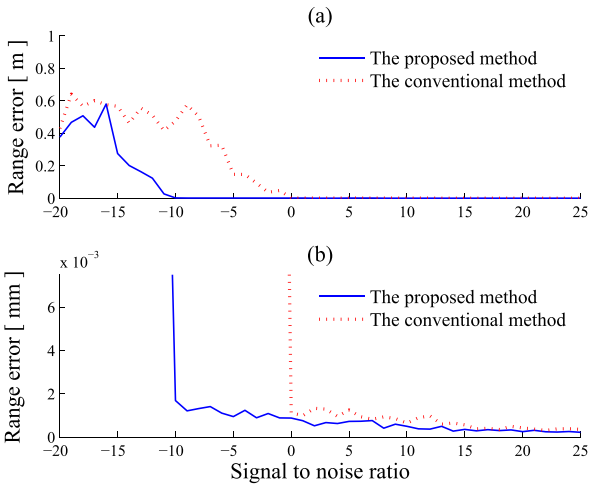

Fig. 12. Influence of noise on the proposed method in which the errors are described by (a) meter and (b) millimeter.

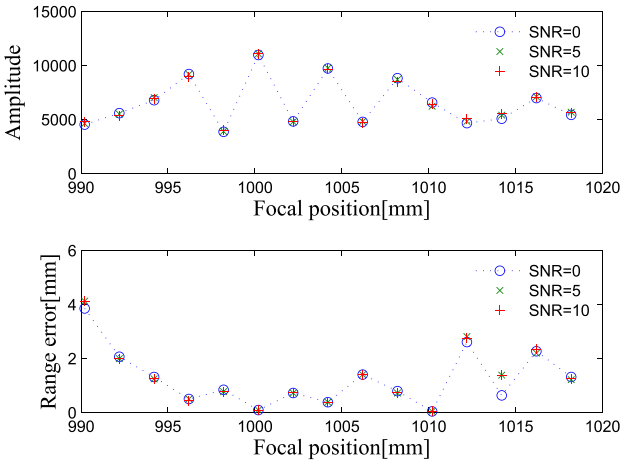

Fig. 13. Relationship between the measuring error and the focal position variation.

always accompanied by noise interference resulting from high air moisture, especially in the region nearing the liquid level. One thing to point out is that the good antinoise performance of our method benefits from the SNR improvement of synthesis signal following the beamforming.

For the examination of influence of focal position on the proposed method, we still use the simulated data of the static liquid-level above. In this verification, we mainly consider the variation of focal position along the scanning direction when the synthesized ultrasound beam samples the liquid level. For the sake of simplicity, we only consider the scanning direction overlapping with the z-axis of transducer array. The relationship between the sampling error and the focal position variation is shown in Fig. 13. In the meantime, we also vary the SNR of received signal in this section.

On the basis of Fig. 13, it is clear that the error is smallest and the amplitude of compressed signal is highest when the focal position moves toward the water–air interface. However, it is indicated that the measuring accuracy is not affected by the focal position in a small scope closing the water–air interface. For example, when the focal position locates in the range of 1000 ± 5 mm approximately, the error is small and achieves 0.16 mm. Besides, the range that the measuring accuracy is not affected when reducing the SNR of received signal. On the other hand, this paper also verifies that the established rule of focal position searching mentioned above is proper. In addition, this rule will ensure the right focal position in DBF adaptively tracking the change of liquid level and achieve the optimal measuring result.

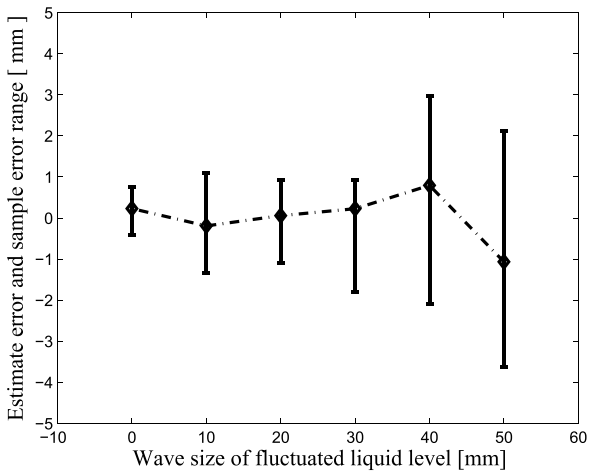

Fig. 14. Level estimate errors and error range of all level samples in every wave size.

Finally, we still evaluate the influence of wave size of liquid level on the proposed method. Toward this end, we implement the simulated measurement of fluctuated liquid level with different wave sizes. Here, we need to note that the wave size refers to the maximum peak of wave. For simplicity, the six sizes of waves are specified in simulations, and they are 0, 10, 20, 30, 40, and 50 mm, respectively. The simulation results are shown in Fig. 14, including the measuring errors of liquid level and the variance of liquid level samples under different wave size conditions.

From Fig. 14, it is observed that the measuring error of fluctuate liquid level will be gradually increased with the increase of wave size. However, the measuring error is very small and nearly invariable when the wave size changes from 0 to 30 mm. Even if the wave size reaches 50 mm, the measuring error is only -1.28 mm. It indicates that the proposed approach can overcome the shortage of the conventional method and achieve an expected measuring error under a certain wave size of liquid-level condition. Unlike the measuring error, the variance of samples is closely linked with the wave size and will increase with the growing of wave size. The latter point means that the terrible error is possible when using the conventional method and ultrasound beam irradiating the peak or valley of fluctuated liquid level.

IV. Verifications Using Real System

A. Setting Up of Real System

We built a real system to verify the feasibility of the method. The real system constitutes three parts: 1) front-end hardware;

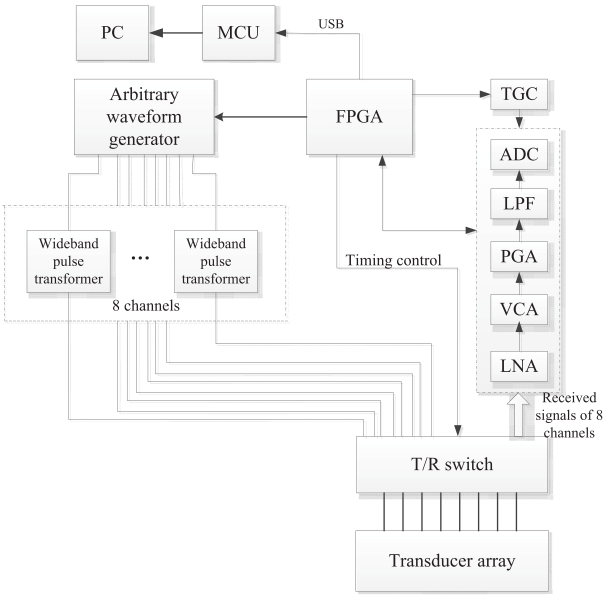

Fig. 15. Block diagram of real system.

2) personal computer (PC) control software; and 3) measuring container. The block diagram of real system is shown in Fig. 15. The front-end hardware mainly consists of the ultrasonic transducer array and the circuit board unit. The transducer array is formed by eight identical circular transducers with a diameter of 12 mm. The central frequency of the transducer is 300 KHz, and the bandwidth is about 120 KHz. According to the transducer array design scheme mentioned above, the formed linear array reaches a length of 282 mm. The transducer array is mounted on the steel support, and its surface vertically faces the liquid level. The circuit board unit includes eight channels of transmitting/receiving (T/R) circuit, T/R switch, arbitrary waveform generator, FPGA, and microcontroller unit (MCU). Under the control of the FPGA, the arbitrary wave generator outputs the FMCW waveform. After being amplified by the wideband pulse transformer, the FMCW signal is sent to the corresponding transmitting transducer. Moreover, the waveform generator can produce other signal waveforms, such as the rectangular pulse, sinusoidal pulse, orthogonal signal, and phase coded signal, so that we can investigate the proposed method using different transmitting signals in our future work. All receiving channels consist of the preamplifier AFE5805, operational amplifier, time gain control amplifier, and analog-to-digital converter. The preamplifier constitutes the low-noise amplifier, voltage-controlled attenuator, programmable gain amplifier, and low-pass filter. The FPGA controls the whole front-end hardware, including waveform generation, signal transmitting/receiving, and data acquisition. Besides, the FPGA still controls the MCU to store data and transfer data to the PC. The front-end hardware is connected to the PC via the universal serial bus. The relevant software written by C++ is to realize the related control function. The point to emphasize here is that the bandwidth of T/R channels is more than 5 MHz. It is designed to allow the further ultrasonic imaging investigation using the proposed method by employing a linear transducer array

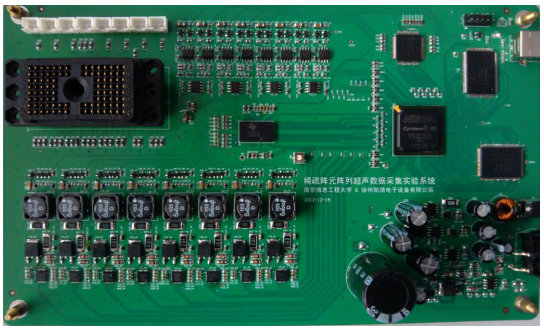

Fig. 16. Developed circuit board of the front-end data acquisition in the real verification system.

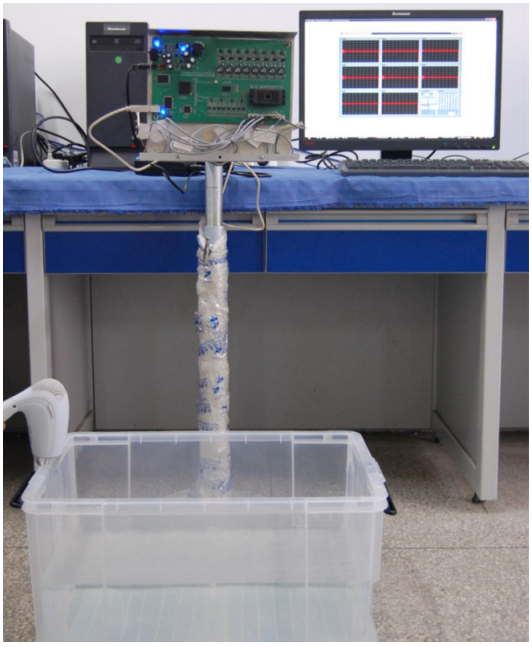

Fig. 17. Complete verification system in actual detection for the dynamic changed liquid level.

with a carry frequency of 3.5 MHz. The photograph of the circuit board unit for the front-end data acquisition is shown in Fig. 16. For simplicity, the measuring container is only a rectangle plastic drum with the size of 0.8 m $\times$ 0.6 m $\times$ 0.5 m. The complete system in experimental measurement is shown in Fig. 17.

B. Detection of Dynamic Liquid Level

We first implement the detection of fluctuated liquid levels where the static level keeps constant. The level fluctuation is formed using a hairdryer to vertically blow the liquid level without interfering with the level measurement. By controlling the wind speed of the hairdryer, two different sizes of waves can be obtained. As a result, the wave size of liquid levels in the strong and weak fluctuation are about 10 and 5 mm, respectively. The range from the transducer array surface to the static liquid level is set as 850 mm, and then the ultrasound radiated zone on liquid level is nearly a rectangular region of 600 mm $\times$ 300 mm according to the angular beam width

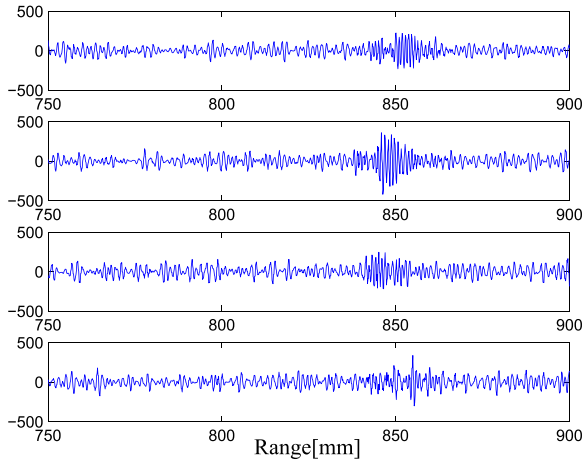

Fig. 18. Real signals received by the virtual transducers.

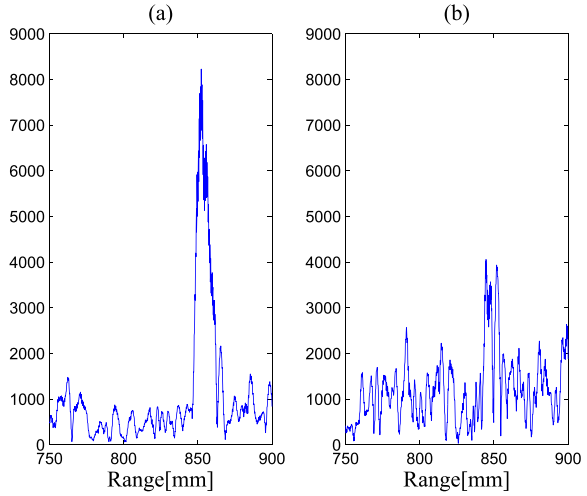

Fig. 19. Pulse compression waveforms of summation signal. (a) With right time delay. (b) Without time delay.

of the ultrasonic transducer. The real signals received by the virtual transducers in the level date collection are shown in Fig. 18. Fig. 19 shows the pulse compression waveforms of summation signal with and without the time delay. The experimental results are in consistent with the simulation ones. The waveforms after the pulse compression made it clear once again that the beamforming technology can improve the SNR of received signal and the most popular method in time domain can meet our requirement. For each wave size, we keep the level detection about every minute, and repeat 20 times in total. The level estimations and the error absolute values are employed to evaluate the proposed method. Besides, the proposed method is compared with the conventional approach as well. To maintain the same experimental conditions for the two methods, we still employ the echo signal of the virtual element $x_{2,1}$ or $x_{3,4}$ to serve as the echo signal received by the conventional approach. The level estimations and their error absolute values provided by two approaches are shown in Fig. 20.

Fig. 20 clearly shows that it does not make much difference in two waved level detections when employing the proposed

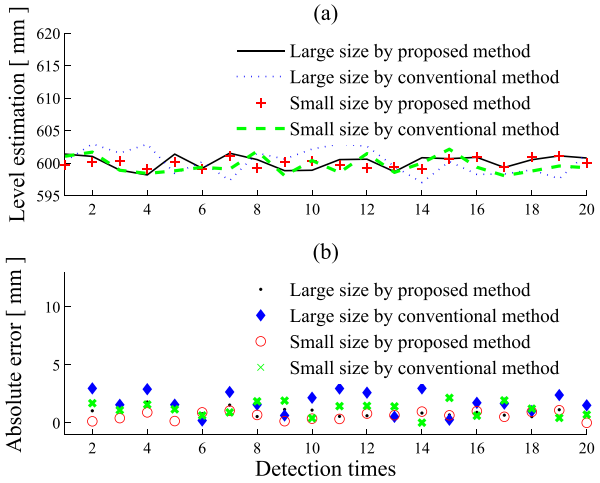

Fig. 20. Level estimations and their absolute errors using two methods for the fluctuated level in different wave size cases, (a) Level estimations and (b)Absolute errors.

approach, and that the maximum error is below 1.2 mm. However, it is another story for the conventional approach. When using the conventional one, the measuring error is likely to increase following the enlargement of wave size, and the maximum error reaches about 3.016 and 4.821 mm individually. Once again, these facts make it clear that the wave size of liquid level has only a much smaller impact on the proposed method. On the other hand, the arithmetic average of level estimations can indicate that the conventional method can get an expected result by repeatedly implementing level detection. However, this simple way may be restricted in our application to the rainfall monitor because the liquid level in the measuring container is randomly changed during rainfall. The verifications of real level measurement demonstrate that our approach is superior to the conventional method in the instantaneous measurement of dynamic liquid levels.

To further verify the reliability of the proposed method in rainfall gauging, it is essential to imitate the dynamic change of liquid level in real environment. First of all, we determine that the maximum rainfall per minute is 38 mm according to the historical meteorological data. Then, we imitate two level changes separately corresponding to torrential and moderate rain. One change is that the liquid level rises 40 mm within 1 min, and the other is 20 mm. In addition to that, we perform one data acquisition every 10% level increase. Meanwhile, the level fluctuation is still produced using the hairdryer to blow the liquid level, and the resulting large and small wave sizes, respectively, correspond to torrential rain and moderate rain. In addition, the water height in the container is fixed as 400 mm, and the starting range from the transducer array surface to the level is 600 mm. In level detection, the actual measured speed of the sound is 349.6 m/s. The results in this simulation of rainfall gauging are shown in Fig. 21. Similarly, the conventional method is compared with the proposed method in this section.

According to Fig. 21, the measuring results are conducive to the proposed method. In the same rainfall condition, the proposed method will always precisely track the change of liquid level, but the conventional method can involve larger

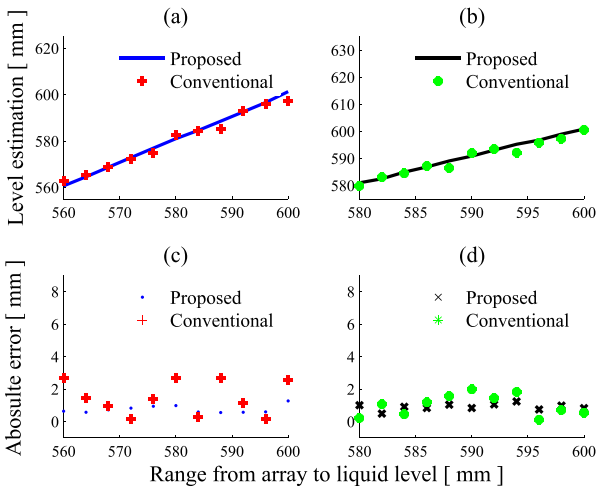

Fig. 21. Testing results following two methods in imitated rainfall gauging. (a) and (b) Level estimation and (c) and (d) absolute errors, respectively, corresponding to the (a) and (c) torrential and (b) and (d) moderate rain.

errors at some liquid levels. It is clear that the maximum absolute errors are, respectively, 1.255 and 3.68 mm, following the proposed and the conventional method in moderate rain condition. Moreover, the maximum errors corresponding to the two methods are 1.276 and 6.28 mm in torrential rain conditions. These experimental results further illustrate that the accuracy of the proposed method can be assured in worst rainfall conditions, while the performance of the conventional method will deteriorate along with rainfall increase. Therefore, this verification not only demonstrates that the proposed method is competent to accurate rainfall gauging in extreme conditions, but also supports once again that the proposed method can prevail over the conventional signal channel method in the determination of dynamic change liquid level.

V. Conclusion

This paper proposes an approach to detect the dynamically changed liquid level with the coherent MIMO ultrasonic system. The relevant aspects of the approach have been summarized, such as physical architecture of MIMO array, signal mode of transmitted FMCW, scheme of signal transmitting and receiving, signal processing, and so on. Although the approach has the similar system architecture with the MIMO detection systems in other subjects, the different signal processing is provided to suit the undulate interface detection of large objective. An adaptive searching method of correct focal position in DBF is proposed according to the amplitude of compression signal. This ensures that every sample on the water–air interface has a small error, and then ensures the high accuracy of the measurement results. On the basis of the virtual element technology, the transducer array is designed to reach our goal reducing the complexity and cost of system to a large extent. Besides, a new simulation method of echo signal from liquid level is also proposed in this paper based on the ultrasonic scattering theory and the boundary-layer theory. By this simulation method of echo signal, the proposed method can be overall verified and evaluated.

The simulated and actual experiments demonstrate that the proposed approach can present the high accuracy in dynamically changed liquid-level case when compared with the conventional signal-channel method. Compared with the scanning method with phased array technology, the approach can provide the advantage of low cost and low complexity. These make it particularly attractive for some other practical applications besides the dynamically changed level detection. In addition, the relevant factors influencing on the proposed approach are investigated by simulations, such as focal position, SNR of received signal, and wave size of liquid level. However, the simulations prove that these factors have less influence on the proposed method than the conventional one.

In the proposed method, an adaptive search of correct focal position in DBF is employed to the high accuracy of every sample on the water–air interface. Because of the dependency on the amplitude of compressed synthesized signal at each potential focus position, this adaptive search of correct focal position maybe affects the real-time property of the proposed approach, but this will be less of a problem using the high-speed electronic chip, designing reasonably the hardware system architecture of signal processing, reducing properly the number of level sample, and so on. For the architecture of transducer array, the virtual element technology can achieve a virtual phased array although other architecture of transducer array can also employed to realize the MIMO detection system. This will be beneficial for overall evaluation of the proposed approach by comparing with the real phased array detection system. In addition, our simulation method of echo signal is quite different to the existing method. The echo signal simulated by our method is move closer to actual received signal from liquid level, which is a new way leading to the research on ultrasonic detection of liquid level, particularly the detection for dynamically changed liquid level. As for the influence factors, the wave size of liquid level should be most considered. In our investigation, when increase of wave size exceeds certain extent, the accuracy of proposed approach will decline obviously. In this case, a simple mechanical device to reduce the wave size of liquid is necessary to assure a reliable precision.

Although our motivation is to improve the accuracy of rainfall gauging by ultrasound, the method is desirable in many promising applications. This MIMO-based ultrasonic transducer array structure does not require mechanical control, thus it can be applied to some environments where it would be improper for the conventional method. For example, the method may be necessary for snow cover in meteorological observations, the river level monitor in flood and disaster prevention, and the bin level indicator in cement and mining industry. Moreover, the measuring accuracy of the proposed method can be further improved by increasing another transducer array in the vertical direction of transducer array.

This proposed method has been verified to achieve a precise detection for dynamic changed liquid level, but this is only a preliminary demonstration. Some aspects related to the proposed method have not been investigated. For instance, what signal processing method can be employed to improve the performance of the proposed method when it is employed

in strong noise and interference environments? In addition, what technique can be used to reduce the range ambiguity due to the velocity and acceleration of the detected objective? These aspects related to the proposed method will be included in our future works.

ACKNOWLEDGMENT

The authors would like to thank B. Feng, K. Kang, and his colleague for developing the data acquisition unit of real testing system. In addition, the authors would like to thank anonymous referees for their invaluable comments and suggestions.

REFERENCES

[1] M. Vogt, "An optimized float for reliable radar tank level measurement in bypass pipes," in *Proc. German Microw. Conf. (GeMIC)*, Mar. 2014, pp. 1–4.

[2] T.-H. Wang, M.-C. Lu, C.-C. Hsu, C.-C. Chen, and J.-D. Tan, "Liquid-level measurement using a single digital camera," *Measurement*, vol. 42, no. 4, pp. 604–610, 2009.

[3] Q. Rong *et al.*, "In-fiber quasi-Michelson interferometer for liquid level measurement with a core-cladding-modes fiber end-face mirror," *Opt. Lasers Eng.*, vol. 57, pp. 53–57, Jun. 2014.

[4] J. E. Antonio-Lopez, D. A. May-Arrioja, and P. LiKamWa, "Fiber-optic liquid level sensor," *IEEE Photon. Technol. Lett.*, vol. 23, no. 23, pp. 1826–1828, Dec. 1, 2011.

[5] W. Wang and F. Li, "Large-range liquid level sensor based on an optical fibre extrinsic Fabry–Pérot interferometer," *Opt. Lasers Eng.*, vol. 52, pp. 201–205, Jan. 2014.

[6] T. Nakagawa, A. Hyodo, K. Kogo, H. Kurata, K. Osada, and S. Oho, "Contactless liquid-level measurement with frequency-modulated millimeter wave through opaque container," *IEEE Sensors J.*, vol. 13, no. 3, pp. 926–933, Mar. 2013.

[7] K. Khalid, I. V. Grozescu, L. K. Tiong, L. T. Sim, and R. Mohd, "Water detection in fuel tanks using the microwave reflection technique," *Meas. Sci. Technol.*, vol. 14, no. 11, p. 1905, 2003.

[8] T. Nakagawa, A. Hyodo, K. Osada, H. Kurata, and S. Oho, "Contactless liquid-level measurement through opaque container using millimeter-wave sensor," in *Proc. IEEE Sensors*, Oct. 2011, pp. 1421–1424.

[9] S. C. Bera, H. Mandal, S. Saha, and A. Dutta, "Study of a modified capacitance-type level transducer for any type of liquid," *IEEE Trans. Instrum. Meas.*, vol. 63, no. 3, pp. 641–649, Mar. 2014.

[10] A. A. Kashi, M. Zamani, and M. Shamshirsaz, "Performance evaluation of PEMC liquid level detection sensors subjected to temperature variation," in *Proc. Symp. Design, Test, Integr., Packag. MEMS/MOEMS (DTIP)*, Apr. 2013, pp. 1–4.

[11] K. Chetpattananondh, T. Tapoanoi, P. Phukpattaranont, and N. Jindapetch, "A self-calibration water level measurement using an interdigital capacitive sensor," *Sens. Actuators A, Phys.*, vol. 209, pp. 175–182, Mar. 2014.

[12] K. V. Santhosh and B. K. Roy, "Design of an adaptive calibration technique based on LSSVM for liquid level measurement," in *Proc. 1st Int. Conf. Emerg. Trends Appl. Comput. Sci. (ICETACS)*, Sep. 2013, pp. 43–47.

[13] M. G. Lorenz, L. Mengibar-Pozo, and M. A. Izquierdo-Gil, "High resolution simultaneous dual liquid level measurement system with CMOS camera and FPGA hardware processor," *Sens. Actuators A, Phys.*, vol. 201, pp. 468–476, Oct. 2013.

[14] M. Meribout, M. Habli, A. Al-Naamany, and K. Al-Busaidi, "A new ultrasonic-based device for accurate measurement of oil, emulsion, and water levels in oil tanks," in *Proc. 21st IEEE Instrum. Meas. Technol. Conf. (IMTC)*, vol. 3. May 2004, pp. 1942–1947.

[15] L. Chen, X. Dong, J. Han, and P. Ye, "Development of a ultrasonic instrument for the sealed container's liquid level measurement," in *Proc. 6th World Congr. Intell. Control Autom. (WCICA)*, vol. 1. 2006, pp. 4972–4976.

[16] V. E. Sakharov, S. A. Kuznetsov, B. D. Zaitsev, I. E. Kuznetsova, and S. G. Joshi, "Liquid level sensor using ultrasonic Lamb waves," *Ultrasonics*, vol. 41, no. 4, pp. 319–322, 2003.

[17] L. Angrisani, A. Baccigalupi, and R. S. L. Moriello, "On the use of unscented Kalman filter for improving ultrasonic time-of-flight measurement," in *Proc. IEEE Instrum. Meas. Technol. Conf. (IMTC)*, vol. 3. May 2005, pp. 1606–1611.

[18] L. Angrisani, A. Baccigalupi, and R. S. L. Moriello, "Ultrasonic time-of-flight estimation through unscented Kalman filter," *IEEE Trans. Instrum. Meas.*, vol. 55, no. 4, pp. 1077–1084, Aug. 2006.

[19] S.-B. Jiang, C.-M. Yang, R.-S. Huang, C.-Y. Fang, and T.-L. Yeh, "An innovative ultrasonic time-of-flight measurement method using peak time sequences of different frequencies: Part I," *IEEE Trans. Instrum. Meas.*, vol. 60, no. 3, pp. 735–744, Mar. 2011.

[20] C.-M. Yang, S.-B. Jiang, D.-Y. Lin, F.-M. Lu, Y.-M. Wu, and T.-L. Yeh, "An innovative ultrasonic time-of-flight measurement method using peak time sequences of different frequencies—Part II: Implementation," *IEEE Trans. Instrum. Meas.*, vol. 60, no. 3, pp. 745–757, Mar. 2011.

[21] J. M. Villladangos *et al.*, "Measuring time-of-flight in an ultrasonic LPS system using generalized cross-correlation," *Sensors*, vol. 11, no. 11, pp. 10326–10342, 2011.

[22] M. R. Hoseini, X. Wang, and M. J. Zuo, "Estimating ultrasonic time of flight using envelope and quasi maximum likelihood method for damage detection and assessment," *Measurement*, vol. 45, no. 8, pp. 2072–2080, 2012.

[23] J. I. S. de Oliveira, S. Y. C. Catunda, A. K. Barros, and J.-F. Naviner, "Multi-layer level measurement using adaptive filtering," in *Proc. IEEE Instrum. Meas. Technol. Conf. (IMTC)*, vol. 1. May 2005, pp. 732–736.

[24] B. Shan, J. Zijian, W. Tong, and L. Haozhe, "Application of online SVR on the dynamic liquid level soft sensing," in *Proc. 25th Chin. Control Decision Conf. (CCDC)*, May 2013, pp. 3003–3007.

[25] Y. Miao and S. Wang, "Small amplitude liquid surface sloshing process detected by optical method," *Opt. Commun.*, vol. 315, pp. 91–96, Mar. 2014.

[26] L. L. I. Frederick, "Ultrasonic fluid level sensing without using a stillwell," U.S. Patent US6 581 459 B1, Jun. 24, 2003.

[27] B. Barshan, "Fast processing techniques for accurate ultrasonic range measurements," *Meas. Sci. Technol.*, vol. 11, no. 1, p. 45, 2000.

[28] Y. Huang, P. V. Brennan, D. Patrick, I. Weller, P. Roberts, and K. Hughes, "FMCW based MIMO imaging radar for maritime navigation," *Prog. Electromagn. Res.*, vol. 115, pp. 327–342, 2011.

[29] J. H. G. Ender and J. Klare, "System architectures and algorithms for radar imaging by MIMO-SAR," in *Proc. IEEE Radar Conf.*, May 2009, pp. 1–6.

[30] J. Li, P. Stoica, and X. Zheng, "Signal synthesis and receiver design for MIMO radar imaging," *IEEE Trans. Signal Process.*, vol. 56, no. 8, pp. 3959–3968, Aug. 2008.

[31] G. Wang and Y.-L. Lu, "Sparse frequency waveform design for MIMO radar," *Prog. Electromagn. Res. B*, vol. 20, pp. 19–32, 2010.

[32] A. Meta, P. Hoogeboom, and L. P. Ligthart, "Signal processing for FMCW SAR," *IEEE Trans. Geosci. Remote Sens.*, vol. 45, no. 11, pp. 3519–3532, Nov. 2007.

[33] A. Ribalta, "Time-domain reconstruction algorithms for FMCW-SAR," *IEEE Geosci. Remote Sens. Lett.*, vol. 8, no. 3, pp. 396–400, May 2011.

[34] R. Gierlich, J. Huttner, A. Ziroff, R. Weigel, and M. Huemer, "A reconfigurable MIMO system for high-precision FMCW local positioning," *IEEE Trans. Microw. Theory Techn.*, vol. 59, no. 12, pp. 3228–3238, Dec. 2011.

[35] G. R. Lockwood, P.-C. Li, M. O'Donnell, and F. S. Foster, "Optimizing the radiation pattern of sparse periodic linear arrays," *IEEE Trans. Ultrason., Ferroelectr., Freq. Control*, vol. 43, no. 1, pp. 7–14, Jan. 1996.

[36] M. L. Lees, "Digital beamforming calibration for FMCW radar," *IEEE Trans. Aerosp. Electron. Syst.*, vol. 25, no. 2, pp. 281–284, Mar. 1989.

[37] J. Benesty, J. Chen, Y. A. Huang, and J. Dmochowski, "On microphone-array beamforming from a MIMO acoustic signal processing perspective," *IEEE Trans. Audio, Speech, Lang. Process.*, vol. 15, no. 3, pp. 1053–1065, Mar. 2007.

[38] R. Demirli, X. Rivenq, Y. D. Zhang, C. Ioana, and M. G. Amin, "MIMO array imaging for ultrasonic nondestructive testing," *Proc. SPIE, Nondestruct. Characterization Compos. Mater., Aerosp. Eng., Civil Infrastruct., Homeland Secur.*, vol. 7983, p. 798338, Apr. 2011.

[39] R. Stirling-Gallacher, Q. Wang, and R. Boehnke, "Beam forming device and method," U. S. Patent 20 120 299 773, Nov. 29, 2012.

[40] M. G. Amin, *Through-the-Wall Radar Imaging*. Boca Raton, FL, USA: CRC Press, 2011.

[41] L. Yun and L. Xiaoping, "The viscous resistance calculation for the trimarans based on the boundary layer theory," in *Proc. Int. Conf. Optoelectron. Image Process. (ICOIP)*, vol. 2. Nov. 2010, pp. 657–661.

[42] S.-T. Chen and M. R. Chatterjee, "A numerical analysis and expository interpretation of the diffraction of light by ultrasonic waves in the Bragg and Raman–Nath regimes using multiple scattering theory," *IEEE Trans. Educ.*, vol. 39, no. 1, pp. 56–68, Feb. 1996.
[43] B. Barshan and R. Kuc, "A bat-like sonar system for obstacle localization," *IEEE Trans. Syst., Man, Cybern.*, vol. 22, no. 4, pp. 636–646, Jul./Aug. 1992.
[44] P. M. Morse and K. U. Ingard, *Theoretical Acoustics*. Princeton, NJ, USA: Princeton Univ. Press, 1968.
[45] S. Singh, *Advanced Sampling Theory with Applications: How Michael' Selected' Amy*, vol. 2. Norwell, MA, USA: Kluwer, 2003.

Peng Li received the B.S. degree in electronic engineering from the Nanjing University of Science and Technology, Nanjing, China, in 1990, the M.S. degree in electronic science and technology from the China University of Mining and Technology, Xuzhou, China, in 2003, and the Ph.D. degree in biomedical engineering from Xi'an Jiaotong University, Xi'an, China, in 2008.

He became a Senior Engineer in 2002. He has been involved in medical instrument-related technology and research since 1990. He is teaching Sensors and Measurement Instrument with the Department of Electronic and Information Engineering, Nanjing University of Information Science and Technology, Nanjing, where he is currently an Associate Professor. His current research interests include measurement of weather conditions, meteorological sensors and instruments, and ultrasonic imaging and related signal processing.

Yulei Cai received the B.S. degree from Ludong University, Yantai, China, in 2012. He is currently pursuing the M.E. degree with the Department of Electronic and Information Engineering, Nanjing University of Information Science and Technology, Nanjing, China.

His current research interests include signal and information processing and MIMO ultrasonic imaging system.

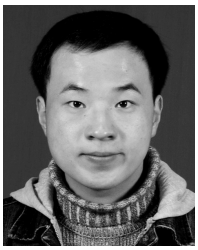

Xiaolong Shen received the B.E. degree from Anhui Jianzhu University, Hefei, China, in 2010. He is currently pursuing the M.E. degree in electronic and information engineering with the Nanjing University of Information Science and Technology, Nanjing, China.

His current research interests include signal and information processing, and ultrasound imaging system.

Sharon Nabuzaale received the B.E. degree from the Nanjing University of Information Science and Technology, Nanjing, China, in 2014, where she plans to go on to the M.E degree.

Her current research interests include signal and information processing and ultrasonic measuring and imaging system.

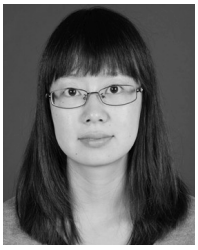

Jie Yin received the B.E. degree from Binjiang College, Nanjing University of Information Science and Technology, Nanjing, China, in 2010, and the M.S. degree in electronic and information engineering from the Nanjing University of Information Science and Technology.

She is currently an Assistant Engineer. Her current research interests include signal and information processing, ultrasound detection and imaging, and software engineering.

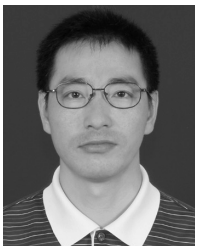

Jiaqiang Li received the B.S. and M.S. degrees in resources and information science from the China University of Petroleum, Qingdao, China, in 2000 and 2003, respectively, and the Ph.D. degree in electronic and electrical engineering from Shanghai Jiao Tong University, Shanghai, China, in 2007.

His current research interests include radar systems and signal processing.